

## Complexation Behavior of Heterocyclic Hydrazones. II. Effects of Steric Factors on Formation Constants for Nickel(II) Complexes with Heterocyclic Hydrazones

Toshiki TAYA, Yukinobu MUKOUYAMA, Kunio DOI, and Makoto OTOMO\*

Department of Applied Chemistry, Nagoya Institute of Technology, Gokiso-cho, Showa-ku, Nagoya 466

(Received September 3, 1993)

The equilibria of nickel(II) ion with thirteen nitrogen-heterocyclic hydrazones (neutral form: HL) with and without blocking group(s) have been investigated spectrophotometrically in 28% aqueous dioxane solution at 25 °C and an ionic strength of 0.2 (KCl). For a series of 2-pyridinecarbaldehyde 5-substituted-2-pyridylhydrazones, the following linear free energy relationships (LFER) were derived between the overall formation constants,  $\beta_1$ ,  $\beta_1'$ , and  $\beta_2$ , of  $\text{Ni}(\text{HL})^{2+}$ ,  $\text{NiL}^+$ , and  $\text{Ni}(\text{HL})_2^{2+}$  complexes, respectively, and the dissociation constants,  $K_{a1}$  and  $K_{a2}$ , of  $\text{H}_3\text{L}^{2+}$  and  $\text{H}_2\text{L}^+$ , respectively:  $\log \beta_1 = 0.95 (\text{p}K_{a1} + \text{p}K_{a2})/2 + 4.60$ ,  $1/2 \log \beta_2 = 0.95 \times (\text{p}K_{a1} + \text{p}K_{a2})/2 + 4.82$ , and  $\log \beta_1' = 1.40 (\text{p}K_{a1} + \text{p}K_{a2})/2 + 9.73$ .

The steric effects of the 6-methyl group in pyridine and the quinolyl ring in place of pyridyl group on the complex formation were evaluated on the basis of LFER. The complex stabilization effect of the pyridyl group substituted for formyl hydrogen was also evaluated for  $\text{Ni}(\text{HL})_2^{2+}$ ,  $\text{Ni}(\text{HL})^{2+}$ , and  $\text{NiL}^+$  complexes. These results together with LFER were discussed in conjunction with the thermodynamic parameters for the formation of  $\text{Ni}(\text{HL})^{2+}$  complex and the ligand field parameters,  $D_q$ , for  $\text{Ni}(\text{HL})^{2+}$  and  $\text{Ni}(\text{HL})_2^{2+}$  complexes.

Although a large number of *NNN*-tridentate heterocyclic hydrazones (HL as a neutral form) have been used as chromogenic reagents in the spectrophotometric determination of divalent transition metal ions,<sup>1,2)</sup> there is only a little information on the complexation behavior, both thermodynamically and kinetically, of these hydrazones including 2-pyridinecarbaldehyde 2-pyridylhydrazone (PAPH), and its analogs.<sup>3–5)</sup>

Irving et al. vigorously studied the equilibria of transition metal ions with 1,10-phenanthroline (phen) and its analogs and discussed the results from a standpoint of the linear free energy relationship (LFER).<sup>6–9)</sup> They plotted the formation constants of substituted-phen complexes against those of phen complexes in logarithmic units and noticed the steric hindrance of 2-methyl and 2-chloro substituents.<sup>7,9)</sup> Sun and Brewer plotted  $\log K_{\text{ML}}$  against  $\text{p}K_a$  for the formation of Ag(I), Cu(II), and Ni(II) complexes with a series of pyridine derivatives,<sup>10)</sup> in which the slopes obtained were not necessarily unity. They associated the magnitude of the slopes and the intercepts with the degree of  $\pi$ -bonding in the systems and further noticed the steric hindrance of 2-methyl and 2-amino substituents.

An abbreviated expression of the structural formula of the ligands examined are shown in Chart 1. These hydrazones are classified into three groups; A, B, and C. The  $R_1$  and  $R_2$  of group A hydrazones are 2-pyridyl, 5-substituted 2-pyridyl, or 1-isoquinolyl rings. The  $R_1$  or/and  $R_2$  of group B hydrazones, that is, 6-methyl-2-pyridyl or/and 2-quinolyl rings, cause a steric hindrance

in complexation with metals. The  $R_3$  of group A and B hydrazones is hydrogen, but the  $R_3$  of group C hydrazones is 2-pyridyl ring.

In this study the formation constants of the nickel(II) complexes with thirteen heterocyclic hydrazones in 28% aqueous dioxane solution were determined. The thermodynamic parameters for the formation of some  $\text{Ni}(\text{HL})^{2+}$  complexes were determined by the temperature-coefficient method. The electronic spectra due to the d–d transitions were measured for  $\text{Ni}(\text{HL})^{2+}$  and  $\text{Ni}(\text{HL})_2^{2+}$  complexes and the ligand-field parameter,  $D_q$ , and the ligand field stabilization energy (LFSE) for these complexes were also obtained. The equilibria of nickel(II) ion with the hydrazones were discussed from a standpoint of LFER together with the thermodynamic parameters and LFSE.

### Experimental

**Reagents and Chemicals.** The thirteen hydrazones studied in this work were PAPH, 2-pyridinecarbaldehyde 5-methyl-2-pyridylhydrazone (PA5MPH), 2-pyridinecarbaldehyde 5-chloro-2-pyridylhydrazone (PA5CPH), 2-pyridinecarbaldehyde 5-nitro-2-pyridylhydrazone (PA5NPH), 1-isoquinolinecarbaldehyde 2-pyridylhydrazone (iQAPH), 2-quinolinecarbaldehyde 2-pyridylhydrazone (QAPH), 2-pyridinecarbaldehyde 2-quinolylhydrazone (PAQH), 2-quinolinecarbaldehyde 2-quinolylhydrazone (QAQH), 6-methylpyridine-2-carbaldehyde 2-pyridylhydrazone (6MPAPH), 6-methylpyridine-2-carbaldehyde 6-methyl-2-pyridylhydrazone (6MPA6MPH), di-2-pyridyl ketone 2-pyridylhydrazone (DPPH), di-2-pyridyl ketone 2-quinolylhydrazone (DPQH), and di-2-pyridyl ketone 5-nitro-2-pyridylhydrazone (DP5NPH), all of which were prepared as described earlier.<sup>11)</sup> Nickel(II) nitrate was dissolved in water containing a small amount of hydrochloric acid and standardized against a  $1 \times 10^{-2}$  M ( $M = \text{mol dm}^{-3}$ ) EDTA solution using murexide as an indicator.

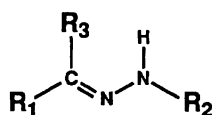


Chart 1.

When necessary, acetic acid, 2-morpholinoethanesulfonic acid, and piperazine-*N,N'*-bis(2-hydroxypropanesulfonic acid) (Dotite Good's buffer) were used combined with hydrochloric acid or potassium hydroxide. Dioxane was freshly distilled before use. All organic and inorganic chemicals were of analytical-reagent grade.

**Methods.** Because of the low solubility of the ligands in water and the mutual comparison of the results, the measurements were mainly done in 28% (v/v) aqueous dioxane solutions of an ionic strength of 0.2 M (KCl) at 25 °C. The acid dissociation constant,  $K_{a3}$ , for the dissociation of imino proton of a ligand was previously determined in aqueous solution by using the  $H_-$  function except for PA5NPH and DP5NPH.<sup>11)</sup> Spectrophotometric and pH measurements were done in the manner described earlier.<sup>11)</sup> The pH readings were corrected by using 28% (v/v) aqueous dioxane solutions of known HCl concentrations ( $3.5 \times 10^{-3}$ – $1.0 \times 10^{-2}$  M) to obtain the hydrogen ion concentrations. All the equilibrium constants determined were therefore the concentration constants. Plot of the values of ( $pK_{a1} + pK_{a2}$ ) or  $\log \beta_1$  in 28% (v/v) aqueous dioxane vs. those in water<sup>12)</sup> gave a straight line with unit slope regardless of ligands used. As described elsewhere,<sup>11)</sup> thermodynamic parameters for the formation of  $Ni(HL)^{2+}$  complexes with several hydrazones were determined by the temperature-coefficient method. Plots of  $\log \beta_1$  against  $1/T$  (8–40 °C) gave good straight lines so that the values of  $\Delta H$  and  $\Delta S$  were obtained from the slope and intercept, respectively, of the equation,  $\log \beta_1 = \Delta H / 2.303RT - \Delta S / 2.303R$ , where  $R$  is the gas constant ( $R = 8.3144 \text{ J K}^{-1} \text{ mol}^{-1}$ ).

**Calculations.** The equilibria of hydrazones with proton or nickel(II) ion are defined in Table 1. As previously described,<sup>12)</sup> the values of unknown constant and molar absorptivity were refined to give the minimum error squares sum,  $U = \sum (A_{i,obs} - A_{i,cal})^2$ , using non-linear regression with the aid of a computer. The goodness-of-fit between  $A_{i,obs}$  and  $A_{i,cal}$  were always checked by using a visualization tool (on a display of the computer) so that the scattering of the deviation of any data points were averaged. The results are tabulated in Table 2. The standard deviation,  $\sigma_i$ , for each  $K_i$  listed in the table is defined as the maximum difference,  $\sigma(K_i) = D_i = \max(K_D - K_{min})_i$ , between the value of  $K_i$  at any point on the "D boundary", introduced by Ingri and Sillén,<sup>13)</sup> and the value,  $K_{min}$ , at the minimum where the "D boundary" corresponds to the  $U$  contour;  $U = U_{min} + U_{min}/(n-m)$  for the number of data points,  $n$ , and the number of unknown constants of  $K_i$ ,  $m$ . For the regression analysis<sup>14)</sup> of equilibrium data, the best straight line through  $x$  and  $y$  coordinates was calculated by minimizing the weighted sum of the squares of the  $x$  and  $y$  residuals. The value of weight,  $\lambda$ , was evaluated by the equation:  $\lambda = (\sigma_x / \sigma_y)^{1/2}$  where the standard deviations of the equilibrium data,  $\sigma_x$  and  $\sigma_y$ , correspond to  $\sigma(K_i)$ .

## Results

The schematic diagram for equilibria of nickel(II) ion with hydrazone is illustrated in Fig. 1. The definition of each equilibrium constant is listed in Table 1.  $K_{a3}$ ,  $K_{a2}$ ,  $K_{a1}$ ,  $K_{c1}$ ,  $K_{c2}$ ,  $K_{ac0}$ ,  $K_{ac1}$ , and  $K_{ac2}$  were all determined spectrophotometrically and  $\beta_1$ ,  $\beta_2$ ,  $\beta_1'$ , and  $\beta_2'$  were obtained by the calculation based on the thermo-

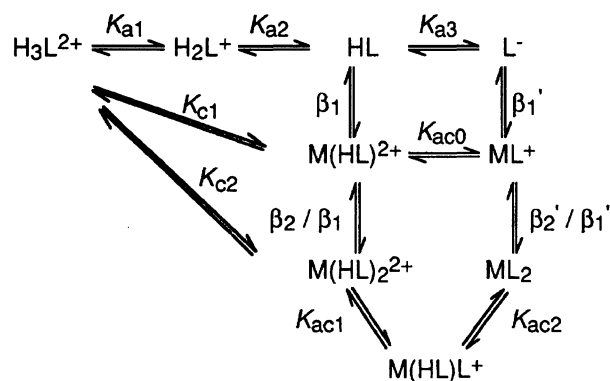


Fig. 1. Scheme for equilibrium relationships between each species of hydrazone in the presence and the absence of nickel(II).

dynamic cycle. The acid dissociation constants,  $K_{a3}$ ,  $K_{a2}$ , and  $K_{a1}$ , of ligand were determined in a similar manner as described elsewhere.<sup>11)</sup>

**Proton Dissociation of 1 : 2 Ni(II)–Hydrazone Complexes.** Nickel(II) ion forms a 1 : 2 complex with hydrazone, HL, in a weakly acid solution containing nickel(II) ion and (5–40)-fold molar excess of hydrazone. Two imino protons of the complex formed successively dissociated with increasing pH, accompanying a significant shift in the absorption maximum from the near ultraviolet to the visible region. The absorbance,  $A$ , of the solution at a wavelength of maximum absorption for  $NiL_2$  is given by

$$A = \epsilon_{c2}[Ni(HL)_2^{2+}] + \epsilon_{c1}[Ni(HL)L^+] + \epsilon_{c0}[NiL_2], \quad (1)$$

where  $\epsilon_{c2}$ ,  $\epsilon_{c1}$ , and  $\epsilon_{c0}$  refer to the molar absorptivities of the species  $Ni(HL)_2^{2+}$ ,  $Ni(HL)L^+$ , and  $NiL_2$ , respectively. The values of  $K_{ac1}$ ,  $K_{ac2}$ ,  $\epsilon_{c2}$ ,  $\epsilon_{c1}$ , and  $\epsilon_{c0}$  were refined by using non-linear regression with the aid of a computer.

**Formation of Ni(II)–Hydrazone Complexes.** For the sake of understanding, the absorption spectra of the ligand and the 1 : 1 and 1 : 2 complexes formed in nickel(II)–DPQH systems, which were recalculated by using all the equilibrium data obtained, are depicted in Fig. 2. Similarly to free ligands, HL,  $H_2L^+$ , and  $H_3L^{2+}$ , the complexes having an undissociated imino proton,  $Ni(HL)^{2+}$ ,  $Ni(HL)L^+$ , and  $Ni(HL)_2^{2+}$ , show an absorption maximum in the near ultraviolet region, shifting to the visible region by the dissociation of the imino proton. The plots of absorbance vs. pH are depicted for 0 : 1 and 1 : 2 molar ratios of nickel(II) to DPQH in Fig. 3. In the plot of the latter molar ratio, a sigmoid curve above pH 3.5 can reasonably be interpreted by two successive proton dissociations, indicating that the imino protons of the  $Ni(HL)_2^{2+}$  complex formed below pH 3.5 dissociate successively with increasing pH. Further, the plots of apparent molar absorptivity vs. pH for varying molar ratios of nickel(II) to DPQH are depicted

Table 1. Equilibria of Ligands and Their Nickel(II) Complexes

Equilibrium	Definition of constant
$\text{H}_3\text{L}^{2+} \rightleftharpoons \text{H}_2\text{L}^+ + \text{H}^+$	$K_{a1} = [\text{H}_2\text{L}^+][\text{H}^+]/[\text{H}_3\text{L}^{2+}]$
$\text{H}_2\text{L}^+ \rightleftharpoons \text{HL} + \text{H}^+$	$K_{a2} = [\text{H}^+][\text{HL}]/[\text{H}_2\text{L}^+]$
$\text{HL} \rightleftharpoons \text{L}^- + \text{H}^+$	$K_{a3} = [\text{L}^-][\text{H}^+]/[\text{HL}]$
$\text{Ni}^{2+} + \text{H}_3\text{L}^{2+} \rightleftharpoons \text{Ni}(\text{HL})_2^{2+} + 2\text{H}^+$	$K_{c1} = [\text{Ni}(\text{HL})_2^{2+}][\text{H}^+]^2/[\text{Ni}^{2+}][\text{H}_3\text{L}^{2+}]$
$\text{Ni}^{2+} + \text{HL} \rightleftharpoons \text{Ni}(\text{HL})_2^{2+}$	$\beta_1 = [\text{Ni}(\text{HL})_2^{2+}]/[\text{Ni}^{2+}][\text{HL}]^a$
$\text{Ni}(\text{HL})_2^{2+} \rightleftharpoons \text{NiL}^+ + \text{H}^+$	$K_{ac0} = [\text{NiL}^+][\text{H}^+]/[\text{Ni}(\text{HL})_2^{2+}]$
$\text{Ni}^{2+} + \text{L}^- \rightleftharpoons \text{NiL}^+$	$\beta_{1'} = [\text{NiL}^+]/[\text{Ni}^{2+}][\text{L}^-]^b$
$\text{Ni}^{2+} + 2\text{H}_3\text{L}^{2+} \rightleftharpoons \text{Ni}(\text{HL})_2^{2+} + 4\text{H}^+$	$K_{c2} = [\text{Ni}(\text{HL})_2^{2+}][\text{H}^+]^4/[\text{Ni}^{2+}][\text{H}_3\text{L}^{2+}]^2$
$\text{Ni}^{2+} + 2\text{HL} \rightleftharpoons \text{Ni}(\text{HL})_2^{2+}$	$\beta_2 = [\text{Ni}(\text{HL})_2^{2+}]/[\text{Ni}^{2+}][\text{HL}]^2^c$
$\text{Ni}(\text{HL})_2^{2+} \rightleftharpoons \text{Ni}(\text{HL})\text{L}^+ + \text{H}^+$	$K_{ac1} = [\text{Ni}(\text{HL})\text{L}^+][\text{H}^+]/[\text{Ni}(\text{HL})_2^{2+}]$
$\text{Ni}(\text{HL})\text{L}^+ \rightleftharpoons \text{NiL}_2 + \text{H}^+$	$K_{ac2} = [\text{NiL}_2][\text{H}^+]/[\text{Ni}(\text{HL})\text{L}^+]$
$\text{Ni}^{2+} + 2\text{L}^- \rightleftharpoons \text{NiL}_2$	$\beta_{2'} = [\text{NiL}_2]/[\text{Ni}^{2+}][\text{L}^-]^2^d$

a)  $\log \beta_1 = \log K_{c1} + pK_{a1} + pK_{a2}$ .b)  $\log \beta_{1'} = \log \beta_1 - pK_{ac0} + pK_{a3}$ .c)  $\log \beta_2 = \log K_{c2} + 2(pK_{a1} + pK_{a2})$ .d)  $\log \beta_{2'} = \log \beta_2 - pK_{ac1} - pK_{ac2} + 2pK_{a3}$ .

Table 2. Equilibrium Constants of Hydrazones and Their Nickel(II) Complexes at 25 °C.

Constants	Ligand						
	1 PAPH	2 PA5MPH	3 PA5CPH	4 PA5NPH	5 iQAPH	6 QAPH	7 PAQH
$pK_{a1}$	2.65±0.01	2.80±0.01	1.42±0.01	-0.45±0.04	3.03±0.01	2.33±0.01	2.33±0.01
$pK_{a2}$	5.27±0.01	5.57±0.01	4.22±0.01	3.59±0.01	5.47±0.01	5.01±0.01	5.60±0.01
$pK_{a3}^a)$	14.8 ±0.04	15.1 ±0.05	14.1 ±0.02	11.15±0.01	14.6 ±0.04	14.1 ±0.02	14.1 ±0.02
$\log K_{c1}$	0.37±0.02	0.16±0.02	1.86±0.02	2.86±0.04	0.12±0.02	-0.68±0.02	-0.86±0.02
$\log K_{c2}$	0.90±0.02	0.85±0.02	3.82±0.02	—	1.14±0.02	-1.09±0.04	-0.98±0.03
$pK_{ac0}$	7.68±0.05	8.38±0.03	7.54±0.03	5.41±0.03	7.63±0.04	7.52±0.03	7.11±0.04
$pK_{ac1}$	7.08±0.01	7.34±0.01	6.10±0.01	—	6.29±0.01	5.83±0.01	5.64±0.01
$pK_{ac2}$	8.50±0.01	8.77±0.01	7.51±0.01	—	7.81±0.01	7.53±0.01	7.41±0.01
$\log \beta_1$	8.29±0.02	8.53±0.02	7.50±0.02	6.00±0.04	8.62±0.02	6.66±0.02	7.08±0.02
$\log \beta_2$	16.7 ±0.0	17.6 ±0.0	15.1 ±0.0	—	18.1 ±0.0	13.6 ±0.0	14.9 ±0.0
$\log (\beta_2/\beta_1^2)$	0.12	0.54	0.10	—	0.86	0.28	0.73
$\log \beta_{1'}$	15.4 ±0.1	15.3 ±0.0	14.0 ±0.0	11.8 ±0.0	15.6 ±0.0	13.2 ±0.0	14.1 ±0.0
$\log \beta_{2'}$	30.8 ±0.0	31.7 ±0.0	29.7 ±0.0	—	33.3 ±0.0	28.4 ±0.0	30.1 ±0.0
$\log (\beta_{2'}/\beta_{1'}^2)$	0.0	1.1	1.7	—	2.1	2.0	1.9

Constants	Ligand					
	8 QAQH	9 6MPAPH	10 6MPA6MPH	11 DPPH	12 DPQH	13 DP5NPH
$pK_{a1}$	1.96±0.02	3.17±0.01	3.15±0.01	2.51±0.01	2.23±0.01	-0.10±0.04
$pK_{a2}$	5.44±0.01	5.56±0.01	6.06±0.01	4.84±0.01	5.09±0.01	3.38±0.01
$pK_{a3}^a)$	13.7 ±0.02	14.8 ±0.03	15.0 ±0.03	15.4 ±0.06	14.2 ±0.02	11.9 ±0.01
$\log K_{c1}$	-2.88±0.02	-1.10±0.02	-3.54±0.01	1.45±0.02	0.25±0.02	0.12±0.02
$\log K_{c2}$	b)	-1.57±0.03	-7.46±0.01	2.86±0.02	0.91±0.02	1.14±0.04
$pK_{ac0}$	7.29±0.03	8.20±0.04	9.05±0.04	6.48±0.05	6.56±0.05	4.36±0.04
$pK_{ac1}$	b)	6.86±0.01	6.92±0.01	6.40±0.01	4.86±0.01	2.84±0.03
$pK_{ac2}$	6.78±0.03	8.42±0.01	8.81±0.01	8.18±0.01	6.87±0.01	4.15±0.03
$\log \beta_1$	4.52±0.02	7.63±0.02	5.67±0.01	8.80±0.02	7.57±0.02	6.96±0.02
$\log \beta_2$	b)	15.9 ±0.0	11.0 ±0.0	17.6 ±0.0	15.6 ±0.0	12.9 ±0.0
$\log (\beta_2/\beta_1^2)$	—	0.64	-0.34	0.00	0.46	-0.12
$\log \beta_{1'}$	10.9 ±0.0	14.2 ±0.0	11.6 ±0.0	17.7 ±0.1	15.2 ±0.1	14.5 ±0.0
$\log \beta_{2'}$	25.0 ±0.0	30.2 ±0.0	25.2 ±0.0	33.8 ±0.0	32.2 ±0.0	29.7 ±0.1
$\log (\beta_{2'}/\beta_{1'}^2)$	3.2	1.8	2.0	-1.6	1.8	0.7

a)  $pK_{a3}$  was determined by  $H_-$  function in aqueous solution except for PA5NPH and DP5NPH. b)  $\log \beta_2 - pK_{ac1} = 4.35$  (not determined separately because of precipitate).

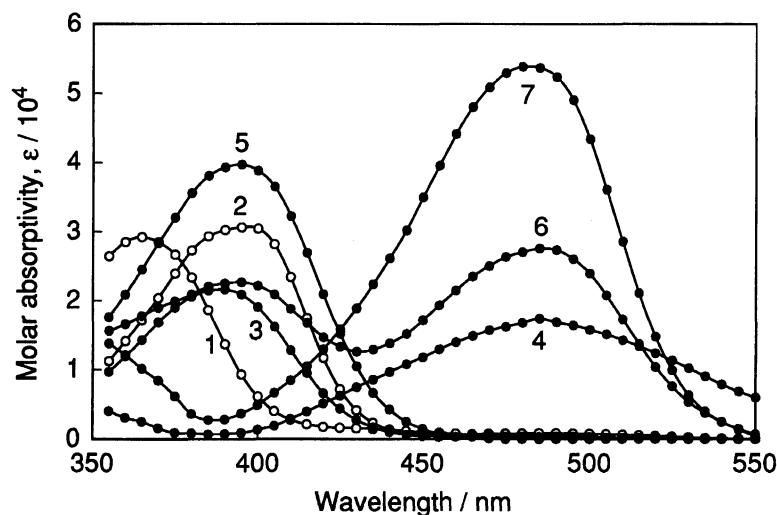


Fig. 2. Calculated molar absorptivities of various species in the system Ni(II)–DPQH as a function of wavelength. ○: ligand (1) HL, (2)  $H_3L^{2+}$ , ●: complex (3)  $Ni(HL)^{2+}$ , (4)  $NiL^+$ , (5)  $Ni(HL)_2^{2+}$ , (6)  $Ni(HL)L^+$ , (7)  $NiL_2$ .

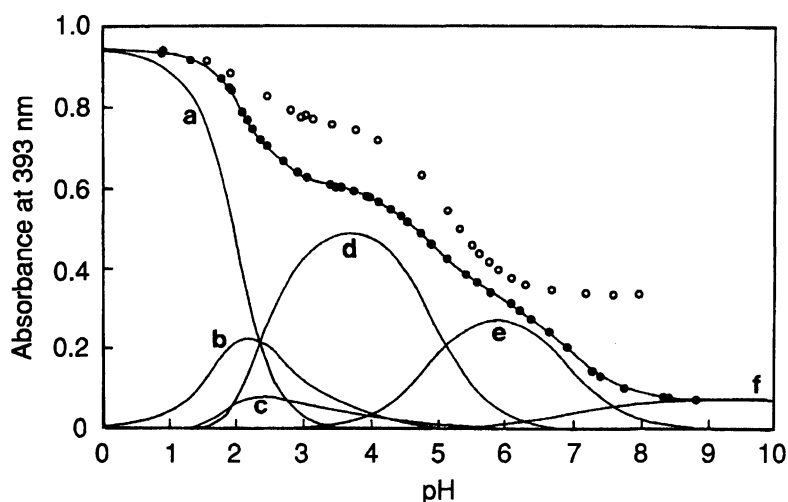


Fig. 3. Absorbance vs. pH plots for DPQH and Ni(II)–DPQH system. Solid lines are calculated curves for each possible species and sum of them. ○:  $C_L = 3.1 \times 10^{-5}$  M; ●:  $C_{Ni} = 1.6 \times 10^{-5}$  M,  $C_L = 3.1 \times 10^{-5}$  M; (a)  $H_3L^{2+}$ , (b)  $H_2L^+$ , (c)  $Ni(HL)^{2+}$ , (d)  $Ni(HL)_2^{2+}$ , (e)  $Ni(HL)L^+$ , (f)  $NiL_2$ .

in Fig. 4, where the plot 1 corresponds to the points, ●, of the plot depicted in Fig. 3. The molar absorptivities of the plateau regions formed at pH 3–4 for the plots 3–5 are obviously different from those for the plots 1 and 2. This supports the idea that a species different from 1:2 complexes, i.e., 1:1 complexes, is formed in the presence of a large excess of nickel(II) ion. Variations of the apparent molar absorptivity at pH 1–3 for the plots 3 and 5 imply the proton dissociation of free ligand together with the complex formation with nickel(II) ion. The sigmoid curve for the plot 5 is superimposed on that for the plot 3, indicating the formation of only one species of complex, i.e.,  $Ni(HL)^{2+}$ . In this pH region, the absorbance,  $A$ , of solution at a wavelength of maximum absorption for  $H_3L^{2+}$  is given by

$$A = \varepsilon_{c1'}[Ni(HL)^{2+}] + \sum \varepsilon_n[H_nL^{(n-1)+}], \quad (2)$$

where  $\varepsilon_{c1'}$  and  $\varepsilon_n$  refer to the molar absorptivities of the species  $Ni(HL)^{2+}$  and  $H_nL^{(n-1)+}$  ( $n=1-3$ ), respectively. The values of  $K_{c1}$  and  $\varepsilon_{c1'}$  were refined by using the known values of  $K_{a1}$ ,  $K_{a2}$ ,  $\varepsilon_1$ ,  $\varepsilon_2$ , and  $\varepsilon_3$ .

For the plots 4 and 5, the sigmoid curves in the pH range 4–8 could not be completely interpreted by a simple acid dissociation of  $Ni(HL)^{2+}$ , suggesting the formation of minute concentrations of 1:2 complexes even in the presence of such a large excess of nickel(II) ion. The formation of 1:2 complexes were confirmed at pH 3.5, 5.1, and 8.1 by the continuous variation method, in which the downward curvatures observed at pH 3.5 and 5.1 in the range of  $C_{Ni}/(C_{Ni} + C_L) > 1/3$  indicate an additional formation of 1:1 complex. Such a downward curvature was not observed at pH 8.1. For the plots 1–5, the following equilibrium is significant in the pH region 5 to 8:

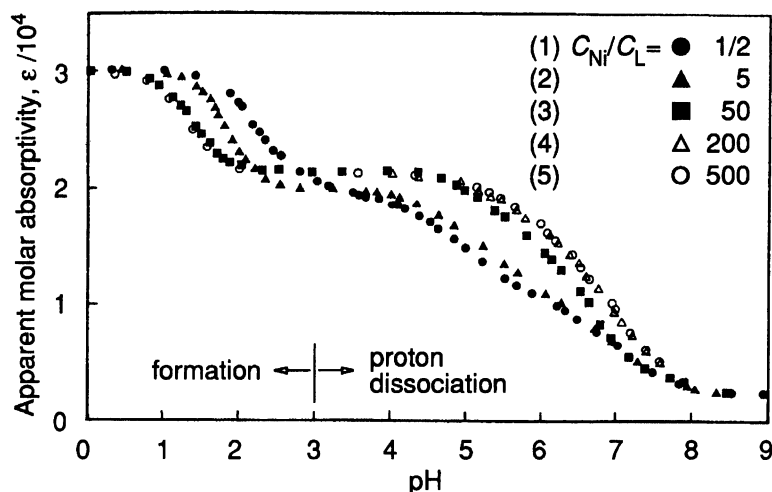
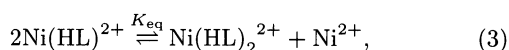


Fig. 4. Apparent molar absorptivity vs. pH plots for Ni(II)-DPQH system with different Ni(II) concentrations. ●,▲,■:  $C_L = 3.2 \times 10^{-5}$  M (with 1-cm cell); △,○:  $C_L = 3.2 \times 10^{-6}$  M (with 10-cm cell).



where  $K_{\text{eq}} = [\text{Ni}(\text{HL})_2^{2+}][\text{Ni}^{2+}]/[\text{Ni}(\text{HL})^{2+}]^2$ . The conditional equilibrium constant,  $K_{\text{eq}}'$ , under the experimental conditions used ( $C_L = 6.2 \times 10^{-6}$  M and  $C_{\text{Ni}} = 5 \times 10^{-5} - 7 \times 10^{-3}$  M at pH 5.53) is defined as  $K_{\text{eq}}' = [\text{Ni}(\text{HL})_2^{2+}][\text{Ni}^{2+}]/[\text{Ni}(\text{HL})']^2$  where  $[\text{Ni}(\text{HL})'] = [\text{Ni}(\text{HL})^{2+}] + [\text{NiL}^+]$  and  $[\text{Ni}(\text{HL})_2'] = [\text{Ni}(\text{HL})_2^{2+}] + [\text{Ni}(\text{HL})\text{L}^+] + [\text{NiL}_2]$ . The logarithmic expression of the equation for  $K_{\text{eq}}'$  is given by

$$\log \frac{[\text{Ni}(\text{HL})_2']}{[\text{Ni}(\text{HL})']^2} = \log K_{\text{eq}}' - \log [\text{Ni}^{2+}] \quad (4)$$

The plot of the left-hand side of Eq. 4 vs.  $-\log [\text{Ni}^{2+}]$  gave a good straight line, the values of slope and intercept ( $= \log K_{\text{eq}}'$ ) being 1.00 and 1.14, respectively. The value of  $\log K_{\text{eq}}'$  can be evaluated by using the values of pH and several equilibrium constants listed in Table 2. The evaluated value of 1.10 is in good agreement with the value of the intercept.

As mentioned for the plot 1, two imino protons of the 1:2 complex,  $\text{Ni}(\text{HL})_2^{2+}$ , formed at pH 1–3 dissociate successively between pH 3 and 8, where the 1:1 complex,  $\text{Ni}(\text{HL})^{2+}$ , is also formed in a small concentration. The concentration of the 1:1 complex decreases with increasing pH of the solution, and thus the proton dissociation of  $\text{Ni}(\text{HL})^{2+}$  can be ignored in the analysis of the plot 1. The absorbance,  $A$ , of solution at a wavelength of maximum absorption for  $\text{H}_3\text{L}^{2+}$  is given by

$$A = \sum \epsilon_n [\text{H}_n\text{L}^{(n-1)+}] + \epsilon_{c1'} [\text{Ni}(\text{HL})^{2+}] + \epsilon_{c2} [\text{Ni}(\text{HL})_2^{2+}] + \epsilon_{c1} [\text{Ni}(\text{HL})\text{L}^+] + \epsilon_{c0} [\text{NiL}_2], \quad (5)$$

where  $n = 1-3$ . The values of  $K_{c2}$ ,  $\epsilon_{c2}$ ,  $\epsilon_{c1}$ , and  $\epsilon_{c0}$  were refined by using the known values of  $K_{a1}$ ,  $K_{a2}$ ,

$K_{c1}$ ,  $K_{ac1}$ ,  $K_{ac2}$ ,  $\epsilon_1$ ,  $\epsilon_2$ ,  $\epsilon_3$ , and  $\epsilon_{c1'}$ . The change in absorbance with pH for each species present in the system is shown in Fig. 3. For the plots 4 and 5 in Fig. 4, the proton dissociation of  $\text{Ni}(\text{HL})^{2+}$  between pH 4 and 8 accompanies a minor formation of  $\text{Ni}(\text{HL})\text{L}^+$  complex, even in the presence of a large excess of nickel(II) ion (cf. Fig. 5). At pH 5–7, about 30–40 h are required to attain the complex formation equilibrium, especially 100–120 h for the PAQH and QAPH systems. The absorbance,  $A$ , of solution at a wavelength of maximum absorption for  $\text{H}_3\text{L}^{2+}$  is given by

$$A = \epsilon_{c1'} [\text{Ni}(\text{HL})^{2+}] + \epsilon_{c0'} [\text{NiL}^+] + \epsilon_{c2} [\text{Ni}(\text{HL})_2^{2+}] + \epsilon_{c1} [\text{Ni}(\text{HL})\text{L}^+] + \epsilon_{c0} [\text{NiL}_2], \quad (6)$$

where  $\epsilon_{c0'}$  is the molar absorptivity of the species  $\text{NiL}^+$ . The values of  $K_{ac0}$  and  $\epsilon_{c0'}$  were refined by using the known values of  $K_{ac1}$ ,  $K_{ac2}$ ,  $\epsilon_{c0}$ ,  $\epsilon_{c1}$ ,  $\epsilon_{c2}$ , and  $\epsilon_{c1'}$ . The formation of a hydrolyzed nickel(II) species,  $\text{Ni}(\text{OH})^+$ ,<sup>15,16</sup> was considered in determining  $K_{ac0}$ . The formation of uncharged bis complex,  $\text{NiL}_2$ , is predominant in weakly basic solution even in the presence of a 500-fold molar excess of nickel(II) ion (cf. Fig. 5).

#### Electronic Spectra due to d-d Transitions for $\text{Ni}(\text{HL})^{2+}$ and $\text{Ni}(\text{HL})_2^{2+}$ Complexes.

Figure 6 shows the electronic absorption spectra of  $\text{Ni}(\text{HL})^{2+}$  complex with PA5MPH, PAPH, and PA5CPH, 1:1 complex with 2,2':6,2''-terpyridine (terpy), and  $\text{Ni}(\text{HL})_2^{2+}$  complex with PAPH. Each spectrum shows a broadened main band in the lowest-energy range. The 1:1 complexes are considered to be present as a form of  $\text{Ni}(\text{HL})(\text{H}_2\text{O})_3^{2+}$  in aqueous solution, the spectra being interpreted on an  $\text{O}_h$  ligand-field model as a first approximation. The main band of each complex is assigned to the spin-allowed transition  ${}^3\text{A}_{2g} \rightarrow {}^3\text{T}_{2g}$ .<sup>17</sup> The wavenumber,  $\nu_{\text{ct}}$ , of the center of the broadened band is  $11240 \text{ cm}^{-1}$  for the complexes with PAPH,

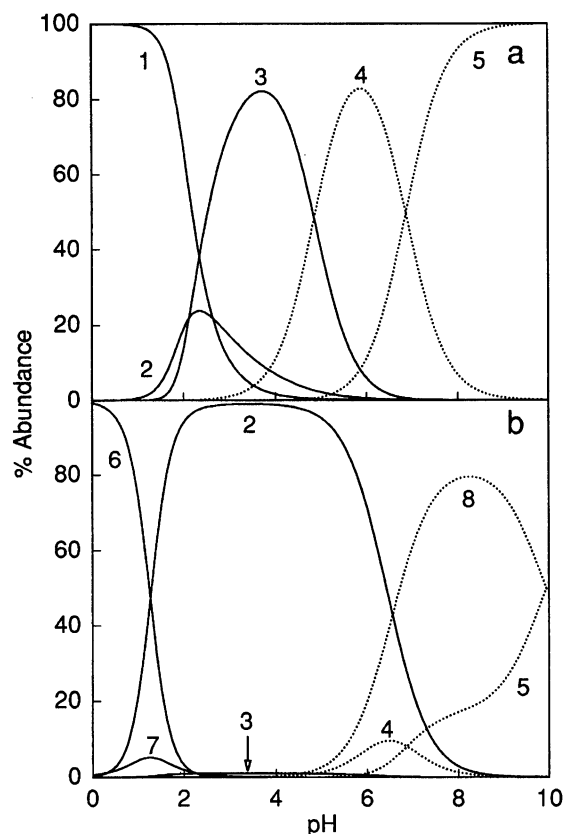


Fig. 5. Distribution diagram of Ni(II)–DPQH system. (a)  $C_L = 3.2 \times 10^{-5}$  M,  $C_{Ni} = 1.6 \times 10^{-5}$  M; (b)  $C_L = 3.2 \times 10^{-6}$  M,  $C_{Ni} = 1.6 \times 10^{-3}$  M; (1)  $Ni^{2+}$ , (2)  $Ni(HL)^{2+}$ , (3)  $Ni(HL)_2^{2+}$ , (4)  $Ni(HL)L^+$ , (5)  $NiL_2$ , (6)  $H_3L^{2+}$ , (7)  $H_2L^+$ , (8)  $NiL^+$ . The dotted lines represent coloring species.

PA5MPH, and PA5CPH and  $11920\text{ cm}^{-1}$  for that with terpy. Each broadened main band is considered as a double-humped band, two peaks of which are located in the range of  $\nu_{ct} \pm 200\text{ cm}^{-1}$ . Similarly the complexes with DPPH and DP5NPH had a broadened band at  $11260 \pm 210$  and  $11290 \pm 210\text{ cm}^{-1}$ , respectively. The spectrum of PA5NPH complex could not be obtained because of the low solubility of the complex. In the cases of the complexes with PA6MPH, 6MPAPH, 6MPA6MPH, and PAQH which bear blocking group(s), the main bands were not broadened, the maximum wavenumbers,  $\nu_{max}$ , being  $10220$ ,  $10220$ ,  $9350$ , and  $10220\text{ cm}^{-1}$ , respectively. Each spectrum of  $Ni(HL)_2^{2+}$  complexes also had a main band without any broadened shape, the  $\nu_{max}$  ( $\text{cm}^{-1}$ ) being:  $12690$  for  $HL = \text{PAPH}$ ;  $12720$  for  $HL = \text{PA5CPH}$ ;  $12010$  for  $HL = 6\text{MPAPH}$ ;  $10990$  for  $HL = 6\text{MPA6MPH}$ ;  $12760$  for  $HL = \text{DPPH}$ ; and  $12680$  for terpy. The wavenumber of  $8550\text{ cm}^{-1}$  was obtained for  $\nu_{max}$  of nickel(II) ion in the aqueous dioxane. The ligand-field parameter,  $D_q$ , was then obtained for each 1:2 complex from the corresponding  $\nu_{max}$  the band of which corresponds to the spin-allowed transition  ${}^3A_{2g} \rightarrow {}^3T_{2g}$ . For each 1:1 complex, the  $D_q$  value

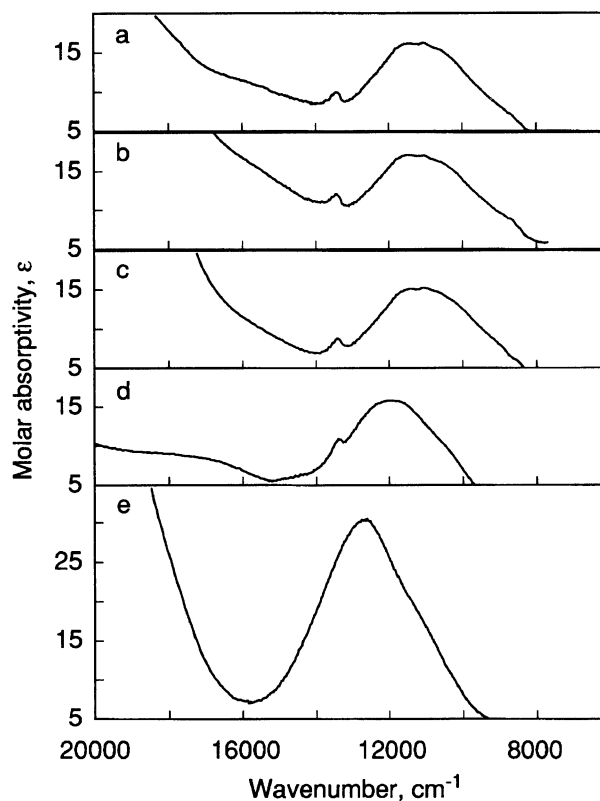


Fig. 6. Electronic absorption spectra of Ni(II) complexes. (a) PA5MPH,  $C_L = 2.5 \times 10^{-3}$  M,  $C_{Ni} = 8.0 \times 10^{-1}$  M; (b) PAPH,  $C_L = 2.6 \times 10^{-3}$  M,  $C_{Ni} = 8.0 \times 10^{-1}$  M; (c) PA5CPH,  $C_L = 2.5 \times 10^{-3}$  M,  $C_{Ni} = 8.0 \times 10^{-1}$  M; (d) terpy,  $C_L = 2.5 \times 10^{-3}$  M,  $C_{Ni} = 8.2 \times 10^{-1}$  M; (e) PAPH,  $C_L = 2.6 \times 10^{-3}$  M,  $C_{Ni} = 1.3 \times 10^{-3}$  M.

was roughly estimated from the corresponding  $\nu_{ct}$  or  $\nu_{max}$ .

### Discussion

Although some equilibrium constants for the nickel(II) complexes with PAPH in aqueous solution have been reported by Green et al.<sup>3)</sup> ( $\log \beta_1 = 8.3$ ,  $\log \beta_2 = 18.5$ ,  $pK_{ac1} = 7.42$ ,  $pK_{ac2} = 8.61$ , and  $\log \beta_2' = 32$  at  $I \approx 0$  and  $25^\circ\text{C}$ ), there are no available data for comparison with ours in aqueous dioxane solution.

All the hydrazones examined act as planar tridentate ligands, their complexing ability being comparable to that of terpy. The distribution diagram for the Ni(II)–DPQH system is shown as a typical example in Fig. 5, characterizing the complexation between nickel(II) ion and a hydrazone with respect to the followings: First, protonated complexes are almost completely formed in fairly acid solution, which are subsequently deprotonated with increasing pH to form colored complexes. The resulting fully deprotonated colored complexes are the most stable of the Ni(II) complexes with *NN*- and *NNN*-multidentate ligands so far reported (cf. Table 2). Second, hydrazone forms pre-

dominantly 1:2 metal to ligand complexes with nickel(II) ion above pH 7 even in the presence of a 500-fold molar excess of nickel(II) ion. As seen from Table 2, the values of  $\log(\beta_2/\beta_1^2)$  and  $\log(\beta_2'/\beta_1'^2)$  are positive for almost all complexes. For the Ni(II) complexes with diethylenetriamine(dien) and terpy as *NNN*-tridentate ligands, the values of  $\log(\beta_2/\beta_1^2)$  are  $-2.4^{18)}$  and  $+0.4^{19)}$  respectively. For heterocyclic ligands such as PAPH and terpy, the successive formation constants of the 1:2 complex are nearly equal or rather large compared with those of the 1:1 complex, which is characteristic of ligands bearing  $sp^2$  hybridized nitrogen(s).<sup>20)</sup> It is very interesting that the trend is maintained even for the complexes with hydrazones bearing blocking groups.

For the complex formation between a particular metal ion and a series of homologous ligands, the formation constant,  $K_{ML}$ , has often been related to the dissociation constant,  $K_a$ , of the ligand:  $\log K_{ML} = a \log K_a + b$ , where  $a$  and  $b$  are constants.<sup>21,22)</sup> The tridentate hydrazones used in this work bear three nitrogens as coordinating atoms, i.e., two heterocyclic nitrogens of  $R_1$  and  $R_2$  and an azomethine nitrogen. As pointed out in a previous paper,<sup>11)</sup> the neutral form, HL, of PAPH is first protonated at the  $R_2$  pyridine-nitrogen while the protonation site is reversed to the  $R_1$  pyridine-nitrogen by the introduction of a strongly electron-withdrawing group such as a chloro or nitro group into the 5-position of  $R_2$  pyridyl ring. It is adequate in a discussion on LFER, therefore, that  $\log \beta_n$  ( $n=1$  and  $2$ ) is plotted against neither  $pK_{a1}$  or  $pK_{a2}$  but  $(pK_{a1} + pK_{a2})/2$ . The plots of  $\log \beta_1$  and  $\log \beta_2$  vs.  $(pK_{a1} + pK_{a2})/2$  are depicted in Fig. 7. Each plot of  $\log \beta_1$  and  $\log \beta_2$  for the 5-substituted PAPH and iQAPH (as group A hydrazones) displays a good straight line. The equations for the lines are given by

$$\log \beta_1 = 0.95 (pK_{a1} + pK_{a2})/2 + 4.60 \quad (7)$$

$$\log \beta_2 = 1.90 (pK_{a1} + pK_{a2})/2 + 9.64, \quad (8)$$

with the absolute correlation coefficients 0.993 and 0.963, respectively. To compare Eq. 8 with Eq. 7, Eq. 8 should be rewritten as:

$$1/2 \log \beta_2 = 0.95 (pK_{a1} + pK_{a2})/2 + 4.82, \quad (9)$$

the slope being equal to that of Eq. 7.

The values of  $\log \beta_1'$  and  $\log \beta_2'$  must be essentially plotted against those of  $(pK_{a1}' + pK_{a2}')/2$  for the proton dissociations of  $R_1$  and  $R_2$  pyridinium groups of the negatively charged species,  $L^-$ , but the  $pK_{a1}'$  values are immeasurable because the species  $L^-$  is first protonated to the imino nitrogen. The values of  $\log \beta_1'$  and  $\log \beta_2'$  are plotted against those of  $(pK_{a1} + pK_{a2})/2$  anyhow in Fig. 8. Similarly to the plots of  $\log \beta_1$ , the plot of  $\log \beta_1'$  for group A displays a good straight line:

$$\log \beta_1' = 1.40 (pK_{a1} + pK_{a2})/2 + 9.73, \quad (10)$$

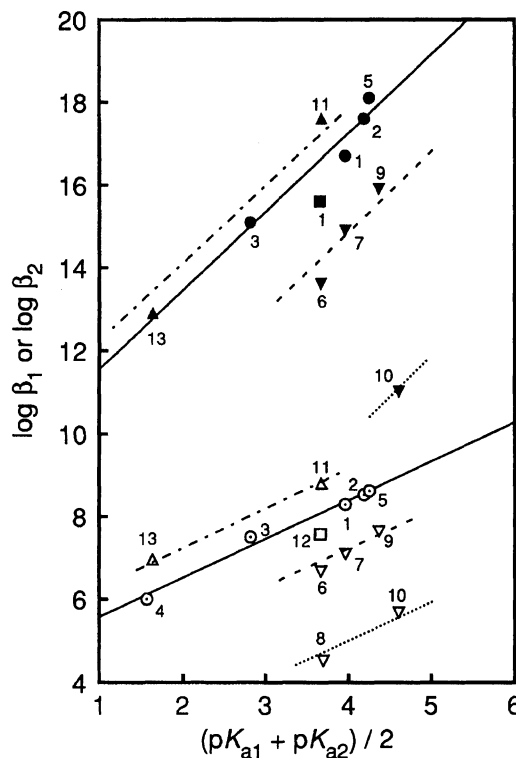


Fig. 7.  $\log \beta_1$  or  $\log \beta_2$  vs.  $(pK_{a1} + pK_{a2})/2$  plots for Ni(II)-hydrazone complexes. Open symbols:  $\log \beta_1$ , Closed symbols:  $\log \beta_2$ .  $\odot, \bullet$ : group A hydrazones,  $\nabla, \blacktriangledown$ : group B hydrazones,  $\triangle, \blacktriangle$ : group C hydrazones. Numbers refer to ligands in Table 2.

with the absolute correlation coefficient of 0.989. This suggests that a linear relationship between  $(pK_{a1} + pK_{a2})$  and  $(pK_{a1}' + pK_{a2}')$  exists in a series of hydrazones having no steric effect in the complexation. On the other hand, the plot of  $\log \beta_2'$  for the complexes with group A hydrazones except for iQAPH displays also a straight line but shows significant scatter.

Sun and Brewer<sup>10)</sup> suggested a relationship ( $\log K_{NiL} = 0.268pK_a + 0.441$ ) between the formation constants of 1:1 Ni(II) complexes with a series of substituted pyridines as monodentate ligands and  $pK_a$  of the ligands. As the hydrazones are tridentate ligands and for comparison with Eqs. 7 and 10, the above relationship should be rewritten as

$$3 \log K_{NiL} = 0.804 pK_a + 1.323. \quad (11)$$

The order of the magnitude of the slopes in Eqs. 7, 10, and 11, is the same as that of  $\log \beta$  of the complexes with the corresponding unsubstituted ligands (pyridine  $< HL < L^-$ ). Although there have been no available data for the complexes with *NN*-bidentate ligands such as 2,2'-bipyridine(bipy) and phen, it is interesting that a larger effect of substituent on complex formation is found in more stable complexes.

In Figs. 7 and 8, the points lying downward of each line of group A hydrazones are considered to form two

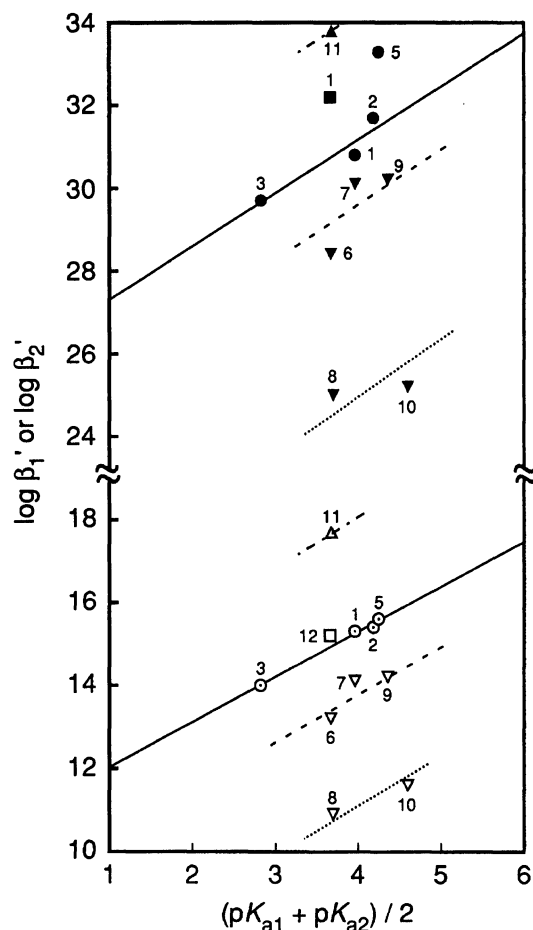


Fig. 8.  $\log \beta_1'$  or  $\log \beta_2'$  vs.  $(pK_{a1} + pK_{a2})/2$  plots for Ni(II)-hydrazone complexes. Open symbols:  $\log \beta_1'$ , Closed symbols:  $\log \beta_2'$ . For  $\log \beta_2'$  solid line was drawn except for iQAPH.  $\circ, \bullet$ : group A hydrazones,  $\nabla, \blacktriangledown$ : group B hydrazones,  $\Delta, \blacktriangle$ : group C hydrazones. Numbers refer to ligands in Table 2.

straight lines roughly parallel to that of group A. These hydrazones, which are classified as group B, bear one or two methyl group(s) adjoining to the donor pyridine-nitrogen atom or one 2-quinolyl group. The 2-quinolyl group of hydrazone also acts as a blocking group in complexation with metals owing to the methine hydrogen atom at 8-position, the extent of destabilization by this group being the same as that by a methyl group. The  $\log \beta$  value of group B hydrazone was smaller than that ( $=\log \beta_{\text{pre}}$ ) predicted from the  $pK_a$  value of the hydrazone according to Eqs. 7 and 8, or 10. The difference ( $\Delta \log \beta = \log \beta - \log \beta_{\text{pre}}$ ) is represented as the destabilization energy ( $\Delta(\Delta G)_{\text{sh}} = -RT \Delta \log \beta$ ). Similarly, the values of  $\Delta(\Delta G)_{\text{sh}}$  was estimated from the distance between the two lines of group A and B hydrazones. The estimated values of  $\Delta(\Delta G)_{\text{sh}}$  of the 1:1 complex,  $\text{Ni}(\text{HL})^{2+}$ , were 6.9 and 19.4  $\text{kJ mol}^{-1}$  for one and two blocking groups in a hydrazone molecule, respectively. In the case of the  $\text{NiL}^+$  complex, the values of 8.3 and 23.1  $\text{kJ mol}^{-1}$  were estimated for one and

two blocking groups, respectively. These values are not much larger than the corresponding values of  $\text{Ni}(\text{HL})^{2+}$  complex. An application of a space-filling model<sup>23)</sup> indicates that a steric hindrance in the formation of a 1:1 complex arises from a steric repulsion between the water molecule coordinated in the *NNN*-plane and the methyl group adjoining to a donor nitrogen atom or the methine hydrogen atom at the 8-position of the quinolyl group. The  $\Delta(\Delta G)_{\text{sh}}$  value for two blocking groups is beyond twice the  $\Delta(\Delta G)_{\text{sh}}$  value for one blocking group, suggesting that these two blocking groups obstructing the entrance of *NNN*-chelate ring multiplicatively enhance the steric hindrance. The values of  $\Delta(\Delta G)_{\text{sh}}$  of the 1:2 complexes,  $\text{Ni}(\text{HL})_2^{2+}$ , were estimated to be 13.7 and 41.4  $\text{kJ mol}^{-1}$  for one and two blocking groups of a hydrazone molecule, respectively. Judging from a space-filling model, a steric hindrance in the 1:2 complex should be caused by a steric repulsion between a blocking group of the coordinated ligand and a part of the second ligand (i.e., the nitrogen atom of azomethine), the cause being definitely different from that for the 1:1 complex.

We have widely used the hydrazones belonging to group C for the spectrophotometric determination of metals and anions<sup>1,24,25)</sup> on the basis of certain analytical advantages such as formation of intensely colored complexes and an appropriate solubility of  $\text{ML}_2$  in organic solvent. In Fig. 7, the points for the 1:1 complexes,  $\text{Ni}(\text{HL})^{2+}$ , with DPPH and DP5NPH lie upward the line for the 1:1 complexes of group A hydrazones. The enhanced stabilization can be attributed to  $\Delta(\Delta G)_{\text{eh}}$ , which is calculated in a similar manner as  $\Delta(\Delta G)_{\text{sh}}$ . The average value of  $\Delta(\Delta G)_{\text{eh}}$  for DPPH and DP5NPH complexes was estimated to be  $-4.0 \text{ kJ mol}^{-1}$ . The two pyridiens bonded to the formyl carbon of ligand restrict mutually their own rotation, which might contribute to the stabilization of the complex by a so-called "preorganization".<sup>20)</sup> The value of  $-3.7 \text{ kJ mol}^{-1}$  was obtained as  $\Delta(\Delta G)_{\text{eh}}$  for the 1:2 complex,  $\text{Ni}(\text{HL})_2^{2+}$ , with DPPH, which corresponds to that of  $-1.9 \text{ kJ mol}^{-1}$  per ligand. The extent of stabilization of the 1:2 complex with group C hydrazones is smaller than that of the 1:1 complex. This cannot be interpreted only by the "preorganization". As mentioned below, the ligand field stabilization energies of 1:1 and 1:2 complexes with DPPH are nearly equal, respectively, to those of 1:1 and 1:2 complexes with PAPH, suggesting that the uncoordinated pyridine of the complexes does not substantially affect the strength of metal-ligand bonds. A space-filling model applied to the 1:1 complex with DPPH suggests the presence of a hydrogen bond or the structure formation of hydration between the uncoordinated pyridine-nitrogen and the water molecule coordinated to the *z* axis in octahedral coordination. The 1:2 complex with DPPH has no advantage in stabilization. The value of  $-16.0 \text{ kJ mol}^{-1}$  was obtained as  $\Delta(\Delta G)_{\text{eh}}$  for the  $\text{NiL}^+$  complex with



DPPH, which is evidently larger than that of the Ni(HL)<sup>2+</sup> complex. The basicity of the uncoordinated pyridine in NiL<sup>+</sup> complex is significantly higher than that in Ni(HL)<sup>2+</sup> complex. This would bring about a further stabilization of the former complex.

The thermodynamic parameters for the formation of Ni(HL)<sup>2+</sup> complexes with PAPH, PA5CPH, and PAQH were determined but those of the PA5NPH complex could not be determined because of the low solubility of HL below 20 °C:  $-\Delta G=47.9$  kJ mol<sup>-1</sup>,  $-\Delta H=42.6$  kJ mol<sup>-1</sup>, and  $T\Delta S=5.3$  kJ mol<sup>-1</sup> for the PAPH complex;  $-\Delta G=42.8$  kJ mol<sup>-1</sup>,  $-\Delta H=35.0$  kJ mol<sup>-1</sup>, and  $T\Delta S=7.8$  kJ mol<sup>-1</sup> for the PA5CPH complex;  $-\Delta G=41.2$  kJ mol<sup>-1</sup>,  $-\Delta H=31.1$  kJ mol<sup>-1</sup>, and  $T\Delta S=10.1$  kJ mol<sup>-1</sup> for the PAQH complex. The results indicate that formation of the 1:1 complex is enthalpy-driven similar to that of most of amine and heterocyclic amine complexes. In comparison with the PAPH complex, the decrease in  $-\Delta G$  for the PA5CPH complex is mainly attributed to the decrease in  $-\Delta H$  resulting from the electron-withdrawing effects of the chloro group. The formation of the PAQH complex is less exothermic and accompanied by a large increase in  $\Delta S$  compared with that of the PAPH complex owing to a steric hindrance of the quinolyl group. This corroborates that the steric hindrance is accompanied by a release of water molecules from 1:1 complex, that is, steric disruption of solvation of the complex by the blocking group.

As shown in Fig. 6b, the electronic spectrum (d-d transition) of the Ni(HL)<sup>2+</sup> complex with PAPH consists of three bands; a broadened main band in the lowest-energy range, a shoulder in a higher-energy range, and probably another band obscured by a much stronger coordinated-ligand absorption. Lions et al.<sup>17)</sup> assigned them to the spin-allowed transition  $^3A_{2g} \rightarrow ^3T_{2g}$  (11100 cm<sup>-1</sup>), the spin-forbidden transition  $^3A_{2g} \rightarrow ^1E_g$  (13500 cm<sup>-1</sup>), and the spin-allowed transition  $^3A_{2g} \rightarrow ^3T_{1g}(F)$  (16500 cm<sup>-1</sup>), respectively, and explained the broadened main band in terms of the rhombic low-symmetry field components. These wavenumbers for the particular d-d transitions agree with ours. The lowest-energy band with a broadened or double-humped shape has been observed for other nickel(II) complexes<sup>26-29)</sup> such as Ni(bipy)<sup>2+</sup>, Ni(en)<sub>3</sub><sup>2+</sup> (en=ethylenediamine), and Ni(phen)<sub>3</sub><sup>2+</sup>.

The value of LFSE for a nickel(II)-hydrazone complex as an octahedral complex was calculated according to the formula:  $\Delta H_{LFSE}=12(D_q(\text{complex})-D_q(\text{hydrate}))$ , where  $D_q(\text{complex})$  and  $D_q(\text{hydrate})$  are the ligand-field parameters for a complex and aqua nickel(II) ion, respectively.<sup>30)</sup> The  $\Delta H_{2LFSE}$  of each 1:2 complex was calculated to be 59.4 kJ mol<sup>-1</sup> for PAPH, 59.8 kJ mol<sup>-1</sup> for PA5CPH, 60.4 kJ mol<sup>-1</sup> for DPPH, 49.7 kJ mol<sup>-1</sup> for 6MPAPH, and 35.0 kJ mol<sup>-1</sup> for 6MPA6MPH. For the N<sub>3</sub>O<sub>3</sub> complex, Ni(HL)(H<sub>2</sub>O)<sub>3</sub><sup>2+</sup>, the value of  $\Delta H_{1LFSE}$  was calculated by

using the approximate  $D_q$  value of the 1:1 complex:  $38.6 \pm 2.4$  kJ mol<sup>-1</sup> for PAPH, PA5MPH, and PA5CPH;  $38.9 \pm 2.5$  kJ mol<sup>-1</sup> for DPPH;  $39.3 \pm 2.5$  kJ mol<sup>-1</sup> for DP5NPH; 23.7 kJ mol<sup>-1</sup> for 6MPAPH, PA6MPH, and PAQH; and 11.5 kJ mol<sup>-1</sup> for 6MPA6MPH. The value of  $\Delta H_{2LFSE}$  of the PA5CPH complex is nearly equal to that of the PAPH complex. Similarly the values of  $\Delta H_{2LFSE}$  of ligands bearing no blocking group are nearly equal to one another. These suggest that an inductive effect by substituent does not so much affect the ligand field of a complex. On the other hand, the introduction of blocking group(s) significantly decreases the value of  $\Delta H_{LFSE}$  indicating that the strain of the bond, induced by blocking group(s), largely influences the ligand field of a complex. The LFSE of a complex is usually related to the enthalpy change,  $\Delta H$ , of formation of the complex. For the PAPH and PAQH complex, the difference between the values of  $\Delta H_{1LFSE}$  is comparable to that of  $-\Delta H$ .

According to the law of average environment,<sup>31)</sup> the values of 10  $D_q$  (cm<sup>-1</sup>) of Ni(HL)(H<sub>2</sub>O)<sub>3</sub><sup>2+</sup> complexes were calculated by using the values of 10  $D_q$  of Ni(HL)<sub>2</sub><sup>2+</sup> and Ni(H<sub>2</sub>O)<sub>6</sub><sup>2+</sup> (=8550 cm<sup>-1</sup>). The differences between experimental and calculated values were: +620 cm<sup>-1</sup> for PAPH; +600 cm<sup>-1</sup> for PA5CPH; +605 cm<sup>-1</sup> for DPPH; -60 cm<sup>-1</sup> for 6MPAPH; and -420 cm<sup>-1</sup> for 6MPA6MPH. The order of the values is compatible with the reverse of the extent of steric hindrance by blocking group(s).

The authors thank Dr. Yutaka Fukuda, Institute for Molecular Science (Okazaki), for his valuable advice in the interpretation of electronic spectra.

## References

- 1) T. Takaoka, T. Taya, and M. Otomo, *Talanta*, **39**, 77 (1992).
- 2) R. B. Singh, P. Jain, and R. P. Singh, *Talanta*, **29**, 77 (1982).
- 3) R. W. Green, P. S. Hallman, and F. Lions, *Inorg. Chem.*, **3**, 376 (1964).
- 4) R. W. Green, P. S. Hallman, and F. Lions, *Inorg. Chem.*, **3**, 1541 (1964).
- 5) R. W. Green and W. G. Goodwin, *Aust. J. Chem.*, **21**, 1165 (1968).
- 6) H. Irving and D. H. Mellor, *J. Chem. Soc.*, **1962**, 5222.
- 7) H. Irving and D. H. Mellor, *J. Chem. Soc.*, **1962**, 5237.
- 8) W. A. E. McBryde, D. A. Brisbin, and H. Irving, *J. Chem. Soc.*, **1962**, 5245.
- 9) H. M. N. H. Irving and P. J. Gee, *Anal. Chim. Acta*, **55**, 315 (1971).
- 10) M. S. Sun and D. G. Brewer, *Can. J. Chem.*, **45**, 2729 (1967).
- 11) T. Taya, T. Sakamoto, K. Doi, and M. Otomo, *Bull. Chem. Soc. Jpn.*, **66**, 3652 (1993).
- 12) T. Taya, T. Ohyabu, K. Doi, and M. Otomo, *Anal.*

*Sci.*, **9**, 835 (1993).

13) N. Ingri and L. G. Sillén, *Ark. Kemi*, **23**, 97 (1964).

14) N. R. Draper and H. Smith, "Applied Regression Analysis," John-Wiley & Sons, New York (1966), Chap. 2.

15) C. F. Baes, Jr., and R. E. Mesmer, "The Hydrolysis of Cations," John-Wiley & Sons, New York (1976), p. 246.

16) T. Kawai, H. Otsuka, and H. Ohtaki, *Bull. Chem. Soc. Jpn.*, **46**, 3753 (1973).

17) F. Lions, I. G. Dance, and J. Lewis, *J. Chem. Soc. A*, **1967**, 565.

18) R. M. Smith and A. E. Martell, "Critical Stability Constants," Plenum Press, New York and London (1975), Vol. 2.

19) A. E. Martell and R. M. Smith, "Critical Stability Constants," Plenum Press, New York and London (1982), Vol. 5.

20) R. D. Hancock and A. E. Martell, *Chem. Rev.*, **89**, 1875 (1989).

21) H. Irving and H. S. Rossotti, *Acta Chem. Scand.*, **10**,

72 (1956).

22) E. Nieboer and W. A. E. McBryde, *Can. J. Chem.*, **48**, 2549 (1970).

23) A. Bondi, *J. Phys. Chem.*, **68**, 441 (1964).

24) T. Kanetake and M. Otomo, *Anal. Sci.*, **4**, 411 (1988).

25) H. Asai, T. Taya, K. Doi, H. Sakamoto, and M. Otomo, *Anal. Sci.*, **7**, 919 (1991).

26) C. K. Jorgensen, *Acta Chem. Scand.*, **9**, 1362 (1955).

27) R. A. Palmer and T. S. Piper, *Inorg. Chem.*, **5**, 864 (1966).

28) R. Dingle and R. A. Palmer, *Theor. Chim. Acta*, **6**, 249 (1966).

29) S. M. Hart, J. C. A. Boeyans, and R. D. Hancock, *Inorg. Chem.*, **22**, 982 (1983).

30) M. Ciampolini, P. Paoletti, and L. Sacconi, *J. Chem. Soc.*, **1960**, 4553.

31) R. D. Hancock and G. J. McDougall, *J. Chem. Soc., Dalton Trans.*, **1977**, 67.